Load Flow Initialization and Dynamic Phasor Modeling of Dual-Stator Winding Induction Machines

T. Tshibungu, A. Masoom, F. Guay
Department of Power System Simulation
Hydro Québec Research Institute, Varennes, Québec, Canada
{tshibungu.tshibain, masoom.alireza, guay.francois2}@hydroquebec.com

***Abstract*— This paper introduces a dynamic phasor (DP)-based modeling for dual-stator winding induction machines (DSIMs), incorporating steady-state formulations to support multiphase load flow initialization. An iterative Newton-Raphson solver is employed to enhance convergence. Under specific assumptions, the DP model exhibits nonlinear characteristics compared to Electromagnetic Transient (EMT)-type models, necessitating iterative solutions for improved accuracy. The proposed DSIM model is validated through EMT-type simulation in HYPERSIM applied to the IEEE 9-bus test system. Benchmarking of transient and load flow simulations confirms that the DP model accurately replicates EMT-type behavior, demonstrating its effectiveness for both dynamic and steady-state analysis of DSIMs.**

***Index Terms*-- Dynamic Phasor, DSIM, Dual Stator Induction Machine, Multiphase Machines, Multiphase Load flow.**

I. INTRODUCTION

Dual stator winding induction machines (DSIMs) have gained attention for their enhanced performance and flexibility in modern electrical drive systems [1]. The stator of the machine is composed of two identical but independent three-phase windings, both designed for the same number of poles. These windings are energized at the same frequency, while the rotor is a conventional squirrel cage type. The two stator windings can be configured in one of two ways. (1): both three-phase windings are accommodated within the same stator and placed with an electrical phase displacement, i.e. 30 degrees, between their magnetic axes, resulting in inherent magnetic coupling. (2): the stator is partitioned so that each three-phase winding occupies only half of the stator. This physical separation renders the magnetic paths independent and effectively eliminates mutual magnetic coupling [3]. The second configuration facilitates advanced control schemes, enhances fault tolerance, and supports multispeed operation. These features make them particularly suitable for applications in industrial drives, electric vehicles, and process industries where precise torque and speed control, and high reliability are critical [2]-[4].

The existing studies on DSIMs focused on developing equivalent models to analyze their steady-state behavior [5]. and dynamic modeling using techniques such as Park's transformation, space vector modeling, and complex vector analysis [6], which allow for accurate simulation of transient responses and control strategies. An EMT-type formulations have been presented in [7]-[8], well-suited for high-resolution transient analysis regardless of whether the mutual coupling between stator windings is considered [9]. Moreover, several studies focus on modeling induction machines using shifted frequency analysis; however, they often lack proper initialization procedures [10].

Dynamic phasor modeling [11] enables efficient simulation of electric machines in steady-state and transient regimes by representing signals as time-varying Fourier coefficients, allowing larger time steps in simulations without compromising numerical stability or computational accuracy. To the authors' knowledge, DP-based models exist for doubly-fed induction generators [12], synchronous machines [13], and other power-system components [14], but no prior work has addressed dynamic phasor modeling of DSIMs.

This paper contributes to an advanced *DP-based model* for DSIM, suitable for both *transient simulation and steady-state multiphase load flow* integration. The model is implemented in C++ using object-oriented principles and validated against EMT-type models within the IEEE 9-bus system using HYPERSIM [15].

II. DYNAMIC PHASOR MODEL OF DSIM

DSIM modeling begins with the abc frame six-phase induction machine formulation [4] assuming sinusoidally distributed stator windings and neglecting inter-stator magnetic coupling, i.e. three-phase winding occupies only half of the stator. Voltage and flux linkage equations are derived in a dq0 synchronous reference frame. For unbalanced operation at the fundamental frequency, the DP model is constructed by: (1) extracting positive, negative, and zero sequences of stator quantities; (2) transforming these to dq0 components; and (3) substituting the superposed dq0 quantities into the machine's differential equations using appropriate Fourier coefficients.

Due to space limitations, the classical dq0 equations are omitted; readers are referred to [8] for the complete formulations and notations. Let f represent a stator or rotor current or voltage signal. Applying the outlined steps, f in the dq0 synchronous reference frame decomposes into DC, fundamental, and double-frequency components, corresponding to positive, negative, and zero sequences. Thus, the relevant DP Fourier coefficients are $k = 0,1,2$. The relation between the instantaneous signal and its DP representation in the dq0 frame rotating at synchronous speed ω_s (denoted by $\langle\ \rangle$) is defined as follows:

979-8-3315-8138-1

$$\mathrm{f}_d = \sum_{k=0,2,-2} \langle \mathrm{f}_d \rangle_k e^{jk\omega_s t} \quad (1)$$

$$\mathrm{f}_q = \sum_{k=0,2,-2} \langle \mathrm{f}_q \rangle_k e^{jk\omega_s t} \quad (2)$$

$$\mathrm{f}_0 = 0.5 \sum_{k=1,-1} \langle \mathrm{f}_0 \rangle_k e^{jk\omega_s t} \quad (3)$$

It's important to note that from (1)-(2), the positive and negative sequences of f; denoted by F_+ and F_-, respectively are obtained as follows:

$$\mathrm{F}_+ = \langle \mathrm{f}_q \rangle_0 - j \langle \mathrm{f}_d \rangle_0 \quad (4)$$

$$\mathrm{F}_- = \langle \mathrm{f}_q \rangle_2 + j \langle \mathrm{f}_d \rangle_2 \quad (5)$$

Substituting (1)-(3) into the classical dq0 equations and ignoring the negative frequency yield the electrical and mechanical equations describing of DSIM in DP (see equations (6)-(23)). In these equations, $*$ denotes the complex conjugate, p represents the derivative operator, the variables related to stator 1, stator 2 and rotor are represented by subscript $s1$, $s2$ and r. The voltage, current and flux are denoted by v, i, φ respectively. The $\mathrm{X}_s^{'}$ and $\mathrm{X}_{ms}^{'}$ are reactance, $\langle \mathrm{E}'_d \rangle_0, \langle \mathrm{E}'_q \rangle_0$ $\langle \mathrm{E}'_d \rangle_2, \langle \mathrm{E}'_q \rangle_2$ are dq transient voltages due to positive and negative sequences, T_r is the rotor time constant. The ω_m and ω_r denote the mechanical and electrical angular speeds (rad/s), p_r is the number of poles, k_d represents the damping coefficient (Nm·s/rad). DP-based torque equation is restricted to two components: constant and the double frequency torques. $\langle \mathrm{T}_{em} \rangle_0$, $\langle \mathrm{T}_{em} \rangle_2$, $\langle \omega_m \rangle_0$, $\langle \omega_m \rangle_2$ are constant and double frequency oscillating torques and speeds, $\langle \mathrm{i}_{ds}^s \rangle_k$, $\langle \mathrm{i}_{qs}^s \rangle_k$ denotes sum of d and q axis stator 1 and 2 currents, respectively.

III. Steady State Equations

If $\langle \omega_m \rangle_2$ is neglected, the positive and negative sequence voltage equations in steady state can be derived using equations (4) and (5). Fig. 1 and Fig. 2 illustrate the equivalent circuits for the positive and negative sequence models of the DSIM. By eliminating the rotor current and applying the Fortescue transformation, the voltage equations are reformulated in the *abc* frame as follows:

$$\begin{bmatrix} \mathbf{V}_{abcs1} \\ \mathbf{V}_{abcs2} \end{bmatrix} = \begin{bmatrix} \mathbf{Z}_{abcs} & \mathbf{Z}_{abcs12} \\ \mathbf{Z}_{abcs21} & \mathbf{Z}_{abcs} \end{bmatrix} \begin{bmatrix} \mathbf{I}_{abcs1} \\ \mathbf{I}_{abcs2} \end{bmatrix} \quad (24)$$

where $\mathbf{Z}_{abcs}$, $\mathbf{Z}_{abcs12}$ and $\mathbf{Z}_{abcs21}$ are impedance matrices, and $\mathbf{V}_{abcs1}$, $\mathbf{V}_{abcs2}$, $\mathbf{I}_{abcs1}$ and $\mathbf{I}_{abcs2}$ are voltage and current vectors in stator 1 and 2 winding. The mechanical and electrical power is computed by:

$$\langle \mathrm{v}_{qs1} \rangle_0 = \mathrm{R}_s \langle \mathrm{i}_{qs1} \rangle_0 + \left(\mathrm{X}_s^{'} \langle \mathrm{i}_{ds1} \rangle_0 + \mathrm{X}_{ms}^{'} \langle \mathrm{i}_{ds2} \rangle_0 + \langle \mathrm{E}_q^{'} \rangle_0 \right) + \tfrac{1}{\omega_s} p \left(\mathrm{X}_s^{'} \langle \mathrm{i}_{qs1} \rangle_0 + \mathrm{X}_{ms}^{'} \langle \mathrm{i}_{qs2} \rangle_0 \right) - \tfrac{1}{\omega_s} p \langle \mathrm{E}_d^{'} \rangle_0 \quad (6)$$

$$\langle \mathrm{v}_{qs2} \rangle_0 = \mathrm{R}_s \langle \mathrm{i}_{qs2} \rangle_0 + \left(\mathrm{X}_s^{'} \langle \mathrm{i}_{ds2} \rangle_0 + \mathrm{X}_{ms}^{'} \langle \mathrm{i}_{ds1} \rangle_0 + \langle \mathrm{E}_q^{'} \rangle_0 \right) + \tfrac{1}{\omega_s} p \left(\mathrm{X}_s^{'} \langle \mathrm{i}_{qs2} \rangle_0 + \mathrm{X}_{ms}^{'} \langle \mathrm{i}_{qs1} \rangle_0 \right) - \tfrac{1}{\omega_s} p \langle \mathrm{E}_d^{'} \rangle_0 \quad (7)$$

$$\langle \mathrm{v}_{ds1} \rangle_0 = \mathrm{R}_s \langle \mathrm{i}_{ds1} \rangle_0 - \left(\mathrm{X}_s^{'} \langle \mathrm{i}_{qs1} \rangle_0 + \mathrm{X}_{ms}^{'} \langle \mathrm{i}_{qs2} \rangle_0 - \langle \mathrm{E}_d^{'} \rangle_0 \right) + \tfrac{1}{\omega_s} p \left(\mathrm{X}_s^{'} \langle \mathrm{i}_{ds1} \rangle_0 + \mathrm{X}_{ms}^{'} \langle \mathrm{i}_{ds2} \rangle_0 \right) + \tfrac{1}{\omega_s} p \langle \mathrm{E}_q^{'} \rangle_0 \quad (8)$$

$$\langle \mathrm{v}_{ds2} \rangle_0 = \mathrm{R}_s \langle \mathrm{i}_{ds2} \rangle_0 - \left(\mathrm{X}_s^{'} \langle \mathrm{i}_{qs2} \rangle_0 + \mathrm{X}_{ms}^{'} \langle \mathrm{i}_{qs1} \rangle_0 - \langle \mathrm{E}_d^{'} \rangle_0 \right) + \tfrac{1}{\omega_s} p \left(\mathrm{X}_s^{'} \langle \mathrm{i}_{ds2} \rangle_0 + \mathrm{X}_{ms}^{'} \langle \mathrm{i}_{ds1} \rangle_0 \right) + \tfrac{1}{\omega_s} p \langle \mathrm{E}_q^{'} \rangle_0 \quad (9)$$

$$p \langle \mathrm{E}_d^{'} \rangle_0 = -\tfrac{1}{\mathrm{T}_r} \left[\langle \mathrm{E}_d^{'} \rangle_0 - \left(\mathrm{X}_s - \mathrm{X}_s^{'} \right) \left(\langle \mathrm{i}_{qs1} \rangle_0 + \langle \mathrm{i}_{qs2} \rangle_0 \right) \right] + \langle \mathrm{E}_q^{'} \rangle_2 \langle \omega_r \rangle_2^{*} + \left(\omega_s - \langle \omega_r \rangle_0 \right) \langle \mathrm{E}_q^{'} \rangle_0 - \langle \omega_r \rangle_2 \langle \mathrm{E}_q^{'} \rangle_2^{*} \quad (10)$$

$$p \langle \mathrm{E}_q^{'} \rangle_0 = -\tfrac{1}{\mathrm{T}_r} \left[\langle \mathrm{E}_q^{'} \rangle_0 - \left(\mathrm{X}_s - \mathrm{X}_s^{'} \right) \left(\langle \mathrm{i}_{ds1} \rangle_0 + \langle \mathrm{i}_{ds2} \rangle_0 \right) \right] + \langle \mathrm{E}_d^{'} \rangle_2 \langle \omega_r \rangle_2^{*} - \left(\omega_s - \langle \omega_r \rangle_0 \right) \langle \mathrm{E}_d^{'} \rangle_0 + \langle \omega_r \rangle_2 \langle \mathrm{E}_d^{'} \rangle_2^{*} \quad (11)$$

$$\langle \mathrm{v}_{qs1} \rangle_2 = \mathrm{R}_s \langle \mathrm{i}_{qs1} \rangle_2 + \left(\mathrm{X}_s^{'} \langle \mathrm{i}_{ds1} \rangle_2 + \mathrm{X}_{ms}^{'} \langle \mathrm{i}_{ds2} \rangle_2 + \langle \mathrm{E}_q^{'} \rangle_2 \right) + j2 \left(\mathrm{X}_s^{'} \langle \mathrm{i}_{qs1} \rangle_2 + \mathrm{X}_{ms}^{'} \langle \mathrm{i}_{qs2} \rangle_2 - \langle \mathrm{E}_d^{'} \rangle_2 \right) - \tfrac{1}{\omega_s} p \langle \mathrm{E}_d^{'} \rangle_2 + \tfrac{1}{\omega_s} p \left(\mathrm{X}_s^{'} \langle \mathrm{i}_{qs1} \rangle_2 + \mathrm{X}_{ms}^{'} \langle \mathrm{i}_{qs2} \rangle_2 \right) \quad (12)$$

$$\langle \mathrm{v}_{qs2} \rangle_2 = \mathrm{R}_s \langle \mathrm{i}_{qs2} \rangle_2 + \left(\mathrm{X}_s^{'} \langle \mathrm{i}_{ds2} \rangle_2 + \mathrm{X}_{ms}^{'} \langle \mathrm{i}_{ds1} \rangle_2 + \langle \mathrm{E}_q^{'} \rangle_2 \right) + j2 \left(\mathrm{X}_s^{'} \langle \mathrm{i}_{qs2} \rangle_2 + \mathrm{X}_{ms}^{'} \langle \mathrm{i}_{qs1} \rangle_2 - \langle \mathrm{E}_d^{'} \rangle_2 \right) - \tfrac{1}{\omega_s} p \langle \mathrm{E}_d^{'} \rangle_2 + \tfrac{1}{\omega_s} p \left(\mathrm{X}_s^{'} \langle \mathrm{i}_{qs2} \rangle_2 + \mathrm{X}_{ms}^{'} \langle \mathrm{i}_{qs1} \rangle_2 \right) \quad (13)$$

$$\langle \mathrm{v}_{ds1} \rangle_2 = \mathrm{R}_s \langle \mathrm{i}_{ds1} \rangle_2 - \left(\mathrm{X}_s^{'} \langle \mathrm{i}_{qs1} \rangle_2 + \mathrm{X}_{ms}^{'} \langle \mathrm{i}_{qs2} \rangle_2 - \langle \mathrm{E}_d^{'} \rangle_2 \right) + j2 \left(\mathrm{X}_s^{'} \langle \mathrm{i}_{ds1} \rangle_2 + \mathrm{X}_{ms}^{'} \langle \mathrm{i}_{ds2} \rangle_2 + \langle \mathrm{E}_q^{'} \rangle_2 \right) + \tfrac{1}{\omega_s} p \langle \mathrm{E}_q^{'} \rangle_2 + \tfrac{1}{\omega_s} p \left(\mathrm{X}_s^{'} \langle \mathrm{i}_{ds1} \rangle_2 + \mathrm{X}_{ms}^{'} \langle \mathrm{i}_{ds2} \rangle_2 \right) \quad (14)$$

$$\langle \mathrm{v}_{ds2} \rangle_2 = \mathrm{R}_s \langle \mathrm{i}_{ds2} \rangle_2 - \left(\mathrm{X}_s^{'} \langle \mathrm{i}_{qs2} \rangle_2 + \mathrm{X}_{ms}^{'} \langle \mathrm{i}_{qs1} \rangle_2 - \langle \mathrm{E}_d^{'} \rangle_2 \right) + j2 \left(\mathrm{X}_s^{'} \langle \mathrm{i}_{ds2} \rangle_2 + \mathrm{X}_{ms}^{'} \langle \mathrm{i}_{ds1} \rangle_2 + \langle \mathrm{E}_q^{'} \rangle_2 \right) + \tfrac{1}{\omega_s} p \langle \mathrm{E}_q^{'} \rangle_2 + \tfrac{1}{\omega_s} p \left(\mathrm{X}_s^{'} \langle \mathrm{i}_{ds2} \rangle_2 + \mathrm{X}_{ms}^{'} \langle \mathrm{i}_{ds1} \rangle_2 \right) \quad (15)$$

$$p \langle \mathrm{E}_d^{'} \rangle_2 = -\tfrac{1}{\mathrm{T}_r} \left[\langle \mathrm{E}_d^{'} \rangle_2 + \left(\mathrm{X}_s - \mathrm{X}_s^{'} \right) \left(\langle \mathrm{i}_{qs1} \rangle_2 + \langle \mathrm{i}_{qs2} \rangle_2 \right) \right] + j2\omega_s \langle \mathrm{E}_d^{'} \rangle_2 + \left(\omega_s - \langle \omega_r \rangle_0 \right) \langle \mathrm{E}_q^{'} \rangle_2 - \langle \omega_r \rangle_2 \langle \mathrm{E}_q^{'} \rangle_0 \quad (16)$$

$$p \langle \mathrm{E}_q^{'} \rangle_2 = -\tfrac{1}{\mathrm{T}_r} \left[\langle \mathrm{E}_q^{'} \rangle_2 - \left(\mathrm{X}_s - \mathrm{X}_s^{'} \right) \left(\langle \mathrm{i}_{ds1} \rangle_2 + \langle \mathrm{i}_{ds2} \rangle_2 \right) \right] - j2\omega_s \langle \mathrm{E}_q^{'} \rangle_2 - \left(\omega_s - \langle \omega_r \rangle_0 \right) \langle \mathrm{E}_d^{'} \rangle_2 + \langle \omega_r \rangle_2 \langle \mathrm{E}_d^{'} \rangle_0 \quad (17)$$

$$\langle \mathrm{v}_{0s1} \rangle_0 = \left(\mathrm{R}_s + j\mathrm{X}_{\sigma s} \right) \langle \mathrm{i}_{0s1} \rangle_1 + \mathrm{l}_{\sigma s} p \langle \mathrm{i}_{0s1} \rangle_1 \quad (18)$$

$$\langle \mathrm{v}_{0s2} \rangle_0 = \left(\mathrm{R}_s + j\mathrm{X}_{\sigma s} \right) \langle \mathrm{i}_{0s2} \rangle_1 + \mathrm{l}_{\sigma s} p \langle \mathrm{i}_{0s2} \rangle_1 \quad (19)$$

$$\mathrm{J} p \langle \omega_m \rangle_0 = \langle \mathrm{T}_{em} \rangle_0 - \langle \mathrm{T}_{load} \rangle_0 - \mathrm{k}_d \langle \omega_m \rangle_0 \quad (20)$$

$$\mathrm{J} \left(p \langle \omega_m \rangle_2 + j2\omega_s \langle \omega_m \rangle_2 \right) = \langle \mathrm{T}_{em} \rangle_2 - \mathrm{k}_d \langle \omega_m \rangle_2 \quad (21)$$

$$\langle \mathrm{T}_{em} \rangle_0 = \frac{-3}{2} \left(\frac{p_r}{2} \right) \frac{\mathrm{L}_{mm}}{\mathrm{L}_{mr}} \left\{ \langle \varphi_{qr} \rangle_0 \langle \mathrm{i}_{ds}^s \rangle_0 - \langle \varphi_{dr} \rangle_0 \langle \mathrm{i}_{qs}^s \rangle_0 + \langle \varphi_{qr} \rangle_2 \langle \mathrm{i}_{ds}^s \rangle_2^{*} - \langle \varphi_{dr} \rangle_2 \langle \mathrm{i}_{qs}^s \rangle_2 - \langle \varphi_{dr} \rangle_2 \langle \mathrm{i}_{qs}^s \rangle_2 \right\} \quad (22)$$

$$\langle \mathrm{T}_{em} \rangle_2 = \frac{-3}{2} \left(\frac{p_r}{2} \right) \frac{\mathrm{L}_{mm}}{\mathrm{L}_{mr}} \left\{ \langle \varphi_{qr} \rangle_0 \langle \mathrm{i}_{ds}^s \rangle_2 + \langle \varphi_{qr} \rangle_2 \langle \mathrm{i}_{ds}^s \rangle_0 - \langle \varphi_{dr} \rangle_0 \langle \mathrm{i}_{qs}^s \rangle_2 - \langle \varphi_{dr} \rangle_2 \langle \mathrm{i}_{qs}^s \rangle_2 - \langle \varphi_{dr} \rangle_2 \langle \mathrm{i}_{qs}^s \rangle_0 \right\} \quad (23)$$

$$
\begin{aligned}
\mathrm{P}_m &= 3(1-s)\Big[a_{pos}\left(\left|\mathrm{I}_{1+}\right|^2+\left|\mathrm{I}_{2+}\right|^2\right)-a_{neg}\left(\left|\mathrm{I}_{1\text{-}}\right|^2+\left|\mathrm{I}_{2\text{-}}\right|^2\right)\Big] \\
&+6(1-s)a_{pos}\begin{bmatrix}\left(\mathrm{I}_{1r+}\mathrm{I}_{2r+}+\mathrm{I}_{1i+}\mathrm{I}_{2i+}\right)\cos\alpha \\ +\left(\mathrm{I}_{1i+}\mathrm{I}_{2r+}-\mathrm{I}_{1r+}\mathrm{I}_{2i+}\right)\sin\alpha\end{bmatrix} \\
&-6(1-s)a_{neg}\begin{bmatrix}\left(\mathrm{I}_{1r\text{-}}\mathrm{I}_{2r\text{-}}+\mathrm{I}_{1i\text{-}}\mathrm{I}_{2i\text{-}}\right)\cos\alpha \\ -\left(\mathrm{I}_{1r\text{-}}\mathrm{I}_{2i\text{-}}-\mathrm{I}_{1i\text{-}}\mathrm{I}_{2r\text{-}}\right)\sin\alpha\end{bmatrix}
\end{aligned}
\tag{25}
$$

$$
\begin{aligned}
\mathrm{P}_e &= 3\mathrm{R}_s\left(\left|\mathrm{I}_{1+}\right|^2+\left|\mathrm{I}_{1\text{-}}\right|^2+\left|\mathrm{I}_{01}\right|^2+\left|\mathrm{I}_{2+}\right|^2+\left|\mathrm{I}_{2\text{-}}\right|^2+\left|\mathrm{I}_{02}\right|^2\right) \\
&+3a_{pos}\left(\left|\mathrm{I}_{1+}\right|^2+\left|\mathrm{I}_{2+}\right|^2\right)+3a_{neg}\left(\left|\mathrm{I}_{1\text{-}}\right|^2+\left|\mathrm{I}_{2\text{-}}\right|^2\right) \\
&+6a_{pos}\begin{bmatrix}\left(\mathrm{I}_{1r+}\mathrm{I}_{2r+}+\mathrm{I}_{1i+}\mathrm{I}_{2i+}\right)\cos\alpha \\ +\left(\mathrm{I}_{1i+}\mathrm{I}_{2r+}-\mathrm{I}_{1r+}\mathrm{I}_{2i+}\right)\sin\alpha\end{bmatrix} \\
&+6a_{neg}\begin{bmatrix}\left(\mathrm{I}_{1r\text{-}}\mathrm{I}_{2r\text{-}}+\mathrm{I}_{1i\text{-}}\mathrm{I}_{2i\text{-}}\right)\cos\alpha \\ +\left(\mathrm{I}_{1r\text{-}}\mathrm{I}_{2i\text{-}}-\mathrm{I}_{1i\text{-}}\mathrm{I}_{2r\text{-}}\right)\sin\alpha\end{bmatrix}
\end{aligned}
\tag{26}
$$

where $a_{pos}=\dfrac{\mathrm{X}_m^2\mathrm{R}_r s}{\mathrm{R}_r^2+\left(s\mathrm{X}_{rr}\right)^2}$ and $a_{neg}=\dfrac{\mathrm{X}_m^2\mathrm{R}_r(2-s)}{\mathrm{R}_r^2+\left((2-s)\mathrm{X}_{rr}\right)^2}$.

The mechanical torque is given by:

$$
\mathrm{T}_m=\frac{p}{2\omega_s}\frac{\mathrm{P}_m}{1-s}
\tag{27}
$$

I_{1+}, $\mathrm{I}_{1\text{-}}$, I_{2+} and $\mathrm{I}_{2\text{-}}$ are stator 1 and 2 positive and negative currents; I_{1r+}, $\mathrm{I}_{1r\text{-}}$ I_{2r+} and $\mathrm{I}_{2r\text{-}}$ are real parts of positive and negative currents in stator 1 and 2; I_{1i+}, $\mathrm{I}_{1i\text{-}}$, I_{2i+} and $\mathrm{I}_{2i\text{-}}$ are imaginary parts of positive and negative sequence currents of stator 1 and 2; and s denotes the slip of DSIM.

IV. Load Flow Equations

One of the following constraint types can be used to characterize the contribution of a DSIM to the load flow analysis: (1): electrical power input, (2): mechanical power, or (3): electromagnetic torque. In this paper, the Modified Augmented Nodal Analysis (MANA) load flow method [16] is employed, utilizing an impedance-based formulation for the participation of the machine. The currents and slip of machine are treated as unknown variables. To incorporate the DSIM into the MANA load flow, the Jacobian matrix is derived from the voltage equations and the selected power or torque constraints. This enables accurate and efficient integration of DSIM behavior into the multiphase flow solution.

A. Voltage equations Contribution into Load flow Matrix

The contribution of voltage equations in the load flow matrix is defined by the function $\mathbf{f}_{IMV}=\mathbf{0}$. The $\mathbf{f}_{IMV}$ is the differential of (24). Therefore, at any given iteration j, we have:

$$
\begin{bmatrix}\Delta\mathbf{V}_{abcs1}\\ \Delta\mathbf{V}_{abcs2}\end{bmatrix}=\begin{bmatrix}\mathbf{Z}_{abcs}^{j} & \mathbf{Z}_{abcs12}^{j}\\ \mathbf{Z}_{abcs21}^{j} & \mathbf{Z}_{abcs}^{j}\end{bmatrix}\begin{bmatrix}\Delta\mathbf{I}_{abcs1}\\ \Delta\mathbf{I}_{abcs2}\end{bmatrix}+\left.\frac{\partial\mathbf{f}_{IMV}}{\partial s}\right|_{s=s^{j}}=-\mathbf{f}_{IMV}^{j}
\tag{28}
$$

B. Additional Constraint of Load flow Matrix

The additional constraint function f_{IM} that contributes to load flow matrix is obtained by setting (25), (26) or (27) to zero

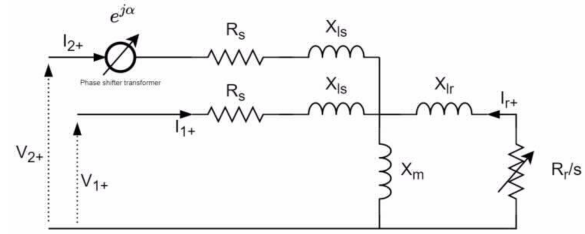

Fig. 1. Positive sequence of DSIM under steady state modeling.

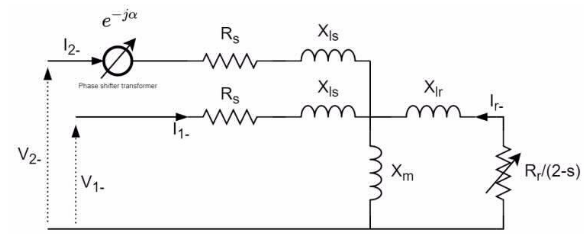

Fig. 2. Negative sequence of DSIM under steady state modeling.

(depending on the constraint type). Thus, at any iteration, we have:

$$
\begin{aligned}
&\left.\frac{\partial\mathbf{f}_{IM}}{\partial\mathrm{I}_{a1\_r}}\right|^{j}\Delta\mathrm{I}_{\mathrm{a1\_r}}+\left.\frac{\partial\mathbf{f}_{IM}}{\partial\mathrm{I}_{b1\_r}}\right|^{j}\Delta\mathrm{I}_{b1\_r}+\left.\frac{\partial\mathbf{f}_{IM}}{\partial\mathrm{I}_{c1\_r}}\right|^{j}\Delta\mathrm{I}_{c1\_r} \\
&+\left.\frac{\partial\mathbf{f}_{IM}}{\partial\mathrm{I}_{a1\_i}}\right|^{j}\Delta\mathrm{I}_{\mathrm{a1\_i}}+\left.\frac{\partial\mathbf{f}_{IM}}{\partial\mathrm{I}_{b1\_i}}\right|^{j}\Delta\mathrm{I}_{\mathrm{b1\_i}}+\left.\frac{\partial\mathbf{f}_{IM}}{\partial\mathrm{I}_{c1\_i}}\right|^{j}\Delta\mathrm{I}_{c1\_i} \\
&+\left.\frac{\partial\mathbf{f}_{IM}}{\partial\mathrm{I}_{a2\_r}}\right|^{j}\Delta\mathrm{I}_{\mathrm{a2\_r}}+\left.\frac{\partial\mathbf{f}_{IM}}{\partial\mathrm{I}_{b2\_r}}\right|^{j}\Delta\mathrm{I}_{\mathrm{b2\_r}}+\left.\frac{\partial\mathbf{f}_{IM}}{\partial\mathrm{I}_{c2\_r}}\right|^{j}\Delta\mathrm{I}_{c2\_r} \\
&+\left.\frac{\partial\mathbf{f}_{IM}}{\partial\mathrm{I}_{a2\_i}}\right|^{j}\Delta\mathrm{I}_{a2\_i}+\left.\frac{\partial\mathbf{f}_{IM}}{\partial\mathrm{I}_{b2\_i}}\right|^{j}\Delta\mathrm{I}_{\mathrm{b2\_i}}+\left.\frac{\partial\mathbf{f}_{IM}}{\partial\mathrm{I}_{c2\_i}}\right|^{j}\Delta\mathrm{I}_{c2\_i} \\
&+\left.\frac{\partial\mathbf{f}_{IM}}{\partial s}\right|^{j}\Delta s=-\mathbf{f}_{IM}^{j}
\end{aligned}
\tag{29}
$$

where I_{a1_r}, I_{b1_r}, I_{c1_r}, I_{a2_r}, I_{b2_r} and I_{c2_r} are real parts of currents in stator 1 and 2; I_{a1_i}, I_{b1_i}, I_{c1_i}, I_{a2_i}, I_{b2_i} and I_{c2_i} are imaginary parts of currents in stator 1 and 2.

V. Time Domain Solution of DP Model

A. EMT-type Formulation of DSIM

The time-domain solution begins by discretizing the electrical and mechanical equations (6)-(23) using the trapezoidal integration method. This leads to the formulation of a companion circuit expressed through nodal equations. To mitigate numerical instability during switching events, a critical damping adjustment technique is applied [17]. The rotor equations are then incorporated into the stator equations to simplify the overall system. By applying the definitions provided in (4) and (5), the positive and negative sequence components of the stator phasors in the rotor reference frame are derived. These components are then transformed using the Fortescue transformation, resulting in an equivalent machine representation in the abc frame.

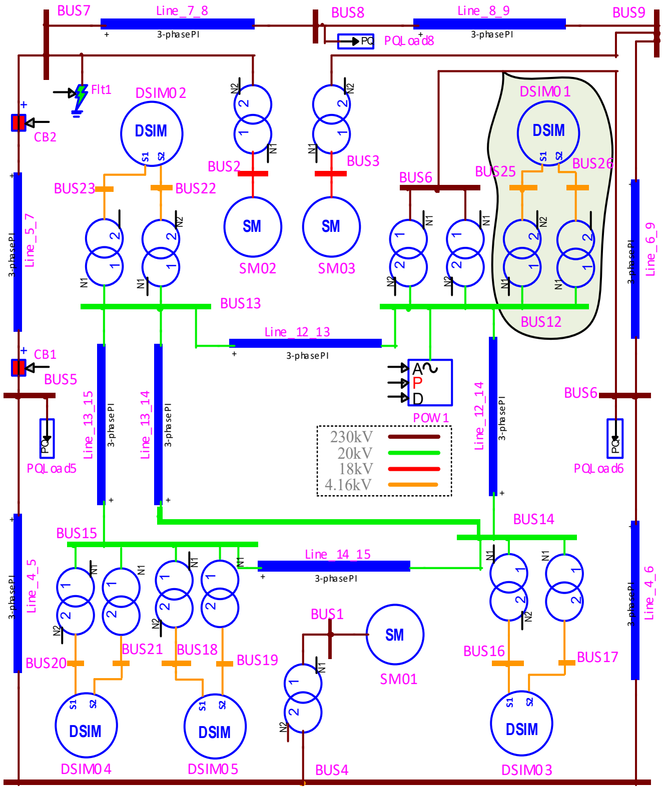

Fig. 3. Diagram of the IEEE 9-bus system implemented in HYPERSIM.

B. *Interfacing DSIM with the main Network*

The positive and negative history terms depend not only on previous time step variables but also on unknown dc speed, double frequency speed, and dq transient voltage at each time point. An easy implementation can be done if the magnitude of $\langle \omega_r \rangle_2$ is negligible under unbalanced conditions. For this study, $\langle \omega_r \rangle_2$ is considered and the coupling and an iterative solution is implemented. The following algorithm summarizes interfacing machine and the main network:

Algorithm

1. Solve DSIMs and get their Norton equivalents,
2. Solve remaining components and get their Norton equivalents,
3. Built the MANA $\mathbf{A}$ matrix and $\mathbf{b}$ vector,
4. Solve $\mathbf{AX_0} = \mathbf{b}$ and go to 4.1
   - 4.1. Solve DSIM as in 1 to update only history terms with unknown variables at instant t
   - 4.2. Solve $\mathbf{AX_1} = \mathbf{b}$
   - 4.3. If $\sqrt{\sum_{i=1}^{N}\left|X_1^{j}(i)-X_0^{j-1}(i)\right|^2} \le \varepsilon$ go to 5 else $\mathbf{X_0} = \mathbf{X_1}$ and go to 4.1.
5. Advance in time $t = t + \Delta t$
6. If $t < t_{\max}$ go to 1 else end simulation

where j is the iteration counter, N is the unknown variables, ε is the smallest number that checks convergence.

VI. Numerical Simulations and Validations

Fig. 3 shows the IEEE-9 bus circuit [18] incorporating five DSIMs, implemented in HYPERSIM [15]. The circuit is fed through three synchronous machines including the controllers. The DSIM model is not available in existing EMT-type tools; therefore, an EMT-type representation was developed in HYPERSIM using the UCM framework. All DSIMs are configured with a "constant power" characteristic, and the breakers CB1 and CB2 at both ends of Line_5_7 are closed. To show the precision of proposed model, it is assumed that a three-phase fault occurs at $t = 0.195\,\text{s}$ on Bus7. The fault is cleared after six cycles by opening the breakers CB1 and CB2. The simulation continues for a total duration of 1.2 s with the time step of 50 µs. All DSIMs in HYPERSIM are initialized using load flow analysis.

A. *Validation of Load flow Solutions*

TABLE I. presents a comparison of load flow results between the DP-based model and the reference, i.e. HYPERSIM for some bus bars. Since the circuit is balanced, results for other phases are omitted. Values from the proposed model are shown in bold, demonstrating high accuracy across most of the circuit. TABLE II. presents a comparison of the power results for the DSIMs obtained from the proposed DP-based model and HYPERSIM. The results are in close agreement, demonstrating the high fidelity and precision of the developed model. The calculated torques and slips are used for the initialization of time-domain solution in the next step.

TABLE I. Comparison of Load flow Results Between Proposed DP-Based DSIM Model (in Bold) and Reference Model, HYPERSIM.

Bus No.	Mag(pu)∟Angle phase-*a*	Bus No.	Mag(pu)∟Angle phase-*a*
BUS01	**1.040 ∟ 0.000** 1.040 ∟0.00	BUS12	**1.007 ∟ -4.238** 1.007 ∟ -4.24
BUS05	**1.025 ∟9.333** 1.026 ∟9.33	BUS13	**1.007∟-4.263** 1.007 ∟ -4.26
BUS15	**1.007 ∟-4.269** 1.007 ∟-4.27	BUS14	**1.007 ∟ -4.263** 1.007 ∟ -4.26

TABLE II. Comparison of Active and Reactive Power Between Proposed DP-Based Model (in Bold) and Reference Model, HYPERSIM.

DSIM No	Ps1 (MW)	Qs1 (MVar)	Ps2 (MW)	Qs2 (MVar)	Tm (kN.m)	Slip (%)
DSIM01	**2.08** 2.08	**1.16** 1.16	**2.08** 2.08	**1.16** 1.16	**21.96**	**2.09**
DSIM02	**2.08** 2.08	**1.16** 1.16	**2.08** 2.08	**1.16** 1.16	**21.96**	**2.09**
DSIM03	**2.08** 2.08	**1.16** 1.16	**2.08** 2.08	**1.16** 1.16	**21.96**	**2.09**
DSIM04	**0.61** 0.61	**0.35** 0.35	**0.61** 0.61	**0.35** 0.35	**6.34**	**0.95**
DSIM05	**0.61** 0.61	**0.35** 0.35	**0.61** 0.61	**0.35** 0.35	**6.34**	**0.95**

B. *Validation of Time-domain Solutions*

Fig. 4.(a) and (b) present the phase-*a* current of stator 1 and stator 2 in DSIM01, respectively. The DP model results are shown in red and green, with the DP envelope emphasized in black, while the HYPERSIM simulation results appear in blue and magenta. As highlighted in the zoomed-in view of the fault and post-fault intervals in Fig. 4 (c), the DP model exhibits a perfect match with the HYPERSIM simulation. Fig. 5 presents a comparison of mechanical torque between the DP model and

979-8-3315-8138-1

HYPERSIM. The two curves show strong agreement, particularly in the fault and post-fault regions highlighted in Fig. 5.(b). Fig. 6 compares the rotor speed of DSIM01, again demonstrating a close match between the DP model and HYPERSIM results, see zoomed-in view of Fig. 6. (b).

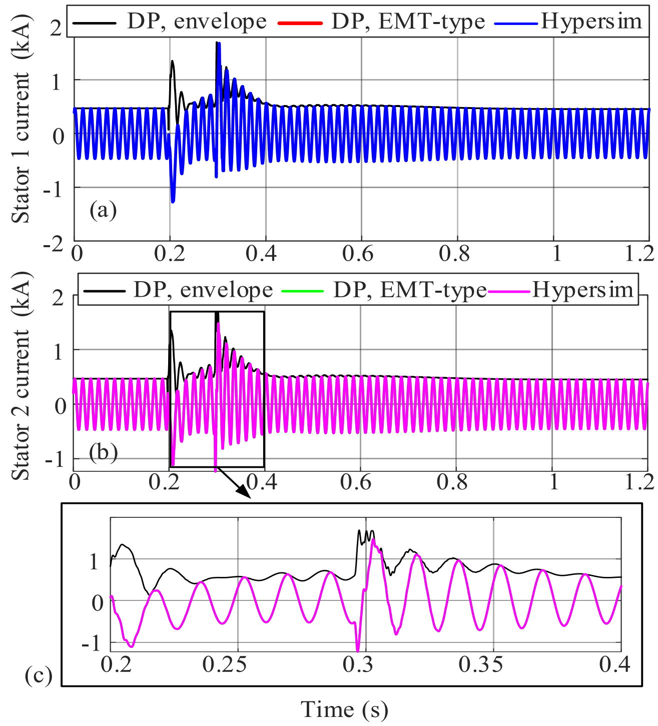

Fig. 4. Phase-a current comparison in DSIM01 between the proposed DP model and the EMT-type model in HYPERSIM: (a) stator 1, (b) stator 2, and (c) zoomed-in view during the fault and post-fault periods.

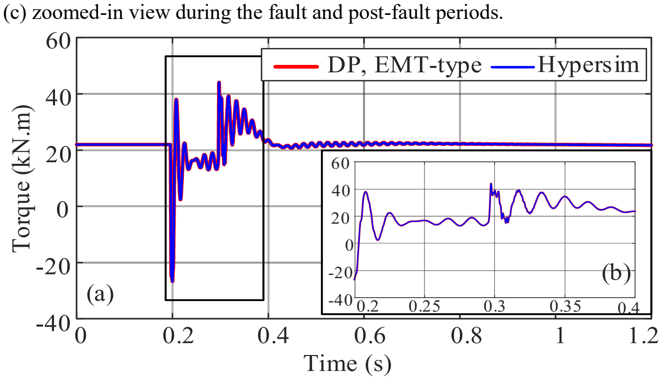

Fig. 5. (a): Comparison of mechanical torque in DSIM01 between the proposed DP model and EMT-type model in HYPERSIM; (b): the zoomed-in view in the fault and post fault period.

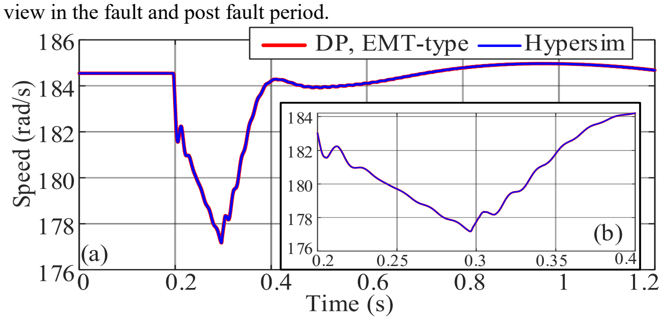

Fig. 6. (a): Rotor speed comparison for DSIM01 between the proposed DP model and EMT-type model in HYPERSIM; (b): the zoomed-in view in the fault and post fault period.

VII. CONCLUSION

This paper presents a dynamic phasor model of the double stator winding induction machine, formulated in the dq synchronous reference frame. The model is applicable under both balanced and unbalanced operating conditions. A corresponding steady-state formulation is derived to facilitate load flow analysis. The implementation is carried out in C++ using object-oriented programming principles, enabling electromagnetic transient type simulations within the dynamic phasor frame. Due to the inherent coupling between positive and negative sequence components, an iterative solution approach is employed to enhance computational accuracy. Simulation results under transient conditions near the system's fundamental frequency validate the model's capability to accurately represent EMT behavior.

REFERENCES

[1] A. R. Munoz and T. A. Lipo, "Dual stator winding induction machine drive," IEEE Transactions on Industry Applications, vol. 36, no. 5, pp. 1369-1379, Sept.-Oct. 2000.

[2] M. Sowmiya, G. Renuka Devi, "Modeling and Control of a Dual Stator Multiphase Induction Motor for Electric Vehicle Technology." Design, Construction, Maintenance, vol. 4, pp. 191-200, 2024.

[3] H. Razik, *Handbook of Asynchronous Machine with Variable Speed*, ISTE Ltd and John Wiley & Sons, 2013, p. 155.

[4] K. Pieńkowski, "Analysis and control of dual stator winding induction motor. Archives of Electrical Engineering", *61*(3), pp. 421-438, 2012.

[5] S. Amachree, D.C. Idoniboyeobu, E.S. Obe & S.L. Braide, "Steady State Analysis of a Dual winding Induction Motor." American Journal of Engineering Research (AJER), vol. 9, Issue 4, pp. 250–255, 2019.

[6] A.S.O. Ogunjuyigbe, T.R. Ayodele, B.B. Adetokun, "Modelling and analysis of dual stator-winding induction machine using complex vector approach," Engineering Science and Technology, an International Journal, vol. 21, pp. 351-363, 2018.

[7] H. Kouki, M.B. Fredj and H. Rehaoulia, "Double stator induction machine modelling: Impact of the stator mutual leakage inductance". International Journal of Applied Electromagnetics and Mechanics, vol. 53, no 1, pp. 51-61, 2017.

[8] T. Tshibungu, "Modeling and Field-Oriented Control of the Dual Stator Winding Induction Motor in the EMTP-Type Environment." Proceedings of International Conference on Power Systems Transients (IPST2015) in Cavtat, Croatia, June 15-18, 2015.

[9] O. Rabiaa, B. H. Mouna, D. Mehdi and S. Lassaad, "Modeling of a dual-three-phase induction motor including the effect of stator mutual leakage inductance," International Conference on Green Energy Conversion Systems (GECS), Hammamet, Tunisia, pp. 1-5, 2017.

[10] P. Zhang, J. R. Marti and H. W. Dommel, "Induction Machine Modeling Based on Shifted Frequency Analysis," IEEE Transactions on Power Systems, vol. 24, no. 1, pp. 157-164, 2009.

[11] D. Turhan. "*Simulation of power system dynamics using dynamic phasor models",* PhD thesis. ETH Zurich, 2008.

[12] B. Braconnier, "Dynamic phasor modeling of doubly-fed induction machines including saturation effects of main flux linkage," master thesis, Univ. of British Columbia, 2012.

[13] R. Hassani, J. Mahseredjian, T. Tshibungu, Ulas Karaagac, "Evaluation of time-domain and phasor-domain methods for power system transients," Electric Power Systems Research, vol. 212, 2022.

[14] R. Hassani, "*Evaluation of Time-Domain and Phasor-Domain Methods for Power System Transients",* Ph.D. thesis, Polytechnique Montréal, 2022.

[15] HYPERSIM, Real-time EMT simulator, [Online Available]: www.opal-rt.com

[16] J. Mahseredjian, "Multiphase load flow method", course notes on power system transients, 2005, Polytechnique Montreal.

[17] J. R. Marti and J. Lin, "Suppression of numerical oscillations in the EMTP," IEEE Trans. Power Systems, vol. 4, no. 2, pp. 739-747, May 1989.

[18] Paul M. Anderson, and Aziz A Fouad, *Power system control and stability*. John Wiley & Sons, 2008.